Journal of Biomolecular NMR, **16:** 253–259, 2000.
KLUWER/ESCOM

Sequential assignment of proline-rich regions in proteins: Application to modular binding domain complexes

Voula Kanelis[a], Logan Donaldson[b], D.R. Muhandiram[b], Daniela Rotin[c], Julie D. Forman-Kay[a] & Lewis E. Kay[b]

[a]*Department of Biochemistry, The University of Toronto and Program in Structural Biology and Biochemistry, The Hospital for Sick Children, Toronto, ON, Canada M5G 1X8*

[b]*Protein Engineering Network Centres of Excellence and Departments of Medical Genetics, Biochemistry and Chemistry, The University of Toronto, Toronto, ON, Canada M5S 1A8*

[c]*Department of Biochemistry, The University of Toronto and Program in Cell Biology, The Hospital for Sick Children, Toronto, ON, Canada M5G 1X8*

Received 13 December 1999; Accepted 10 January 2000

Key words: proline, sequential assignment, triple-resonance NMR

Abstract

Many protein–protein interactions involve amino acid sequences containing proline-rich motifs and even poly-proline stretches. The lack of amide protons in such regions complicates assignment, since ^{1}HN-based triple-resonance assignment strategies cannot be employed. Two such systems that we are currently studying include an SH2 domain from the protein Crk with a region containing 9 prolines in a 14 amino acid sequence, as well as a WW domain that interacts with a proline-rich target. A modified version of the HACAN pulse scheme, originally described by Bax and co-workers [Wang et al. (1995) *J. Biomol. NMR*, **5**, 376–382], and an experiment which correlates the intra-residue $^{1}H^{\alpha}$, $^{13}C^{\alpha}/^{13}C^{\beta}$ chemical shifts with the ^{15}N shift of the subsequent residue are presented and applied to the two systems listed above, allowing sequential assignment of the molecules.

Introduction

Protein–protein interactions regulate a diverse array of cellular processes, including growth and differentiation, motility and enzyme function (Pawson, 1995). With the identification of an increasing number of modular binding domains and associated targets it is apparent that proline-rich sequences play a central role in coordinating many protein complexes. For instance, SH3 domains bind sequences with the minimum consensus PXXP (Yu et al., 1994; Alexandropoulos et al., 1995). A classic example is the interaction of SH3 domains from the adaptor protein Grb2 with the sequence VPPPVPPRR in the guanine nucleotide exchange factor Sos1 (Rozakis-Adcock et al., 1993). WW domains also bind proline-rich regions in their target proteins, of which four types have been identified to date. Three of these contain stretches of sequential proline residues, including XPPXY (Staub et al., 1996; Staub and Rotin, 1996), PPLP (Bedford et al., 1997; Ermekova et al., 1997) and regions rich in P, G and M (Bedford et al., 1998). The newly described GYF domain from the CD2 binding protein CD2BP2 recognizes two tandem repeats of the sequence PPPPGHR spaced seven amino acids apart in the cytoplasmic tail of the T cell surface glycoprotein CD2 (Freund et al., 1999). The cytoskeletal protein profilin binds to the sequence $(P_5G)_3$ as well as stretches of greater than six sequential proline residues (Reinhard et al., 1995; Gertler et al., 1996), while the EVH1 domains in Mena and VASP recognize the core sequence FPPPP found in a number of cytoskeletal proteins (Gertler et al., 1996). A small number of the reported interactions involving poly-Pro sequences are summarized in Table 1.

Over the past several years our laboratories have studied a number of complexes where one of the com-

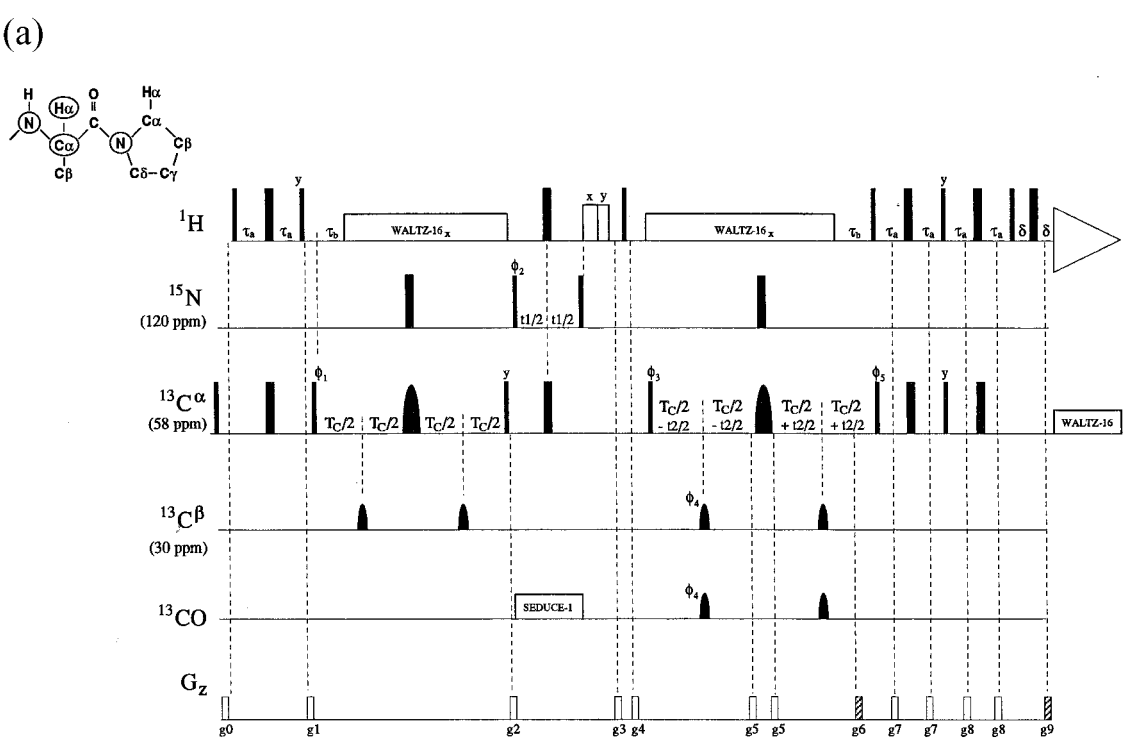

Figure 1. Pulse schemes used to record the HACAN (a) and (HB)CBCA(CO)N(CA)HA (b,c) data sets along with schematic representations of the correlations along the peptide backbone observed in these experiments. All narrow (wide) pulses are applied with a flip angle of 90° (180°) along the x-axis unless indicated otherwise. All ^{1}H and ^{15}N pulses are applied with fields of 31 and 6.5 kHz, respectively, with the exception of ^{1}H WALTZ-16 decoupling (Shaka et al., 1983) (6.5 kHz) and the ^{1}H purge pulses (12.4 kHz, durations of 6 and 3.7 ms for pulses of phase x and y, respectively). (a) All ^{13}C$^\alpha$ rectangular pulses are applied with a 20 kHz field, centered at 58 ppm, while the shaped ^{13}C$^\alpha$ refocusing pulses have the RE-BURP profile (350 μs) (Geen and Freeman, 1991) and are centered at 40 ppm. The ^{13}C$^\beta$ inversion pulses applied during the first $2T_C$ period have the I-BURP2 shape (1.8 ms × 500/ν_o, where ν_o is the spectrometer frequency in MHz, centered at 30 ppm) as do the ^{13}C$^\beta$/^{13}CO pulses (1.8 ms × 500/ν_o) during the second $2T_C$ interval. In the latter case the pulses are applied simultaneously using a waveform obtained by summing phase modulated pulses centered at the ^{13}C$^\beta$ and ^{13}CO regions. ^{13}CO decoupling during t_1 is achieved using a 118 ppm cosine modulated WALTZ scheme where each of the 90° pulses has the SEDUCE-1 shape (345 μs) (McCoy & Mueller, 1992b). ^{13}C$^\alpha$ decoupling during acquisition is achieved using a 2.3 kHz WALTZ field. The delays used are: τ_a = 1.6 ms, τ_b = 3.57 ms, T_C = 11.6 ms, δ = 0.75 ms. The phase cycling is: ϕ1 = (y,−y), ϕ2 = 2(x),2(−x), ϕ3 = 8(x),8(−x), ϕ4 = 4(x),4(−x), ϕ5 = x, rec = 2(x,−x,−x,x),2(−x,x,x,−x). Quadrature detection in t_1 is obtained by States-TPPI (Marion et al., 1989) of ϕ2, while quadrature detection in t_2 is generated using the enhanced sensitivity gradient approach (Kay et al., 1992; Schleucher et al., 1993) where for each value of t_2 data sets with (g6,ϕ5) and (−g6,ϕ5 + 180°) are recorded. For each complex t_2 point the phase ϕ3 and the phase of the receiver are incremented by 180°. The durations and strengths of gradients are: g0 = (1 ms, −5 G/cm), g1 = (0.5 ms, −1 G/cm), g2 = (0.4 ms, −8 G/cm), g3 = (7 ms, 15 G/cm), g4 = (4 ms, 15 G/cm), g5 = (0.3 ms, 12 G/cm), g6 = (1.5 ms, 30 G/cm), g7 = (0.3 ms, 2 G/cm), g8 = (0.4 ms, 2.5 G/cm), g9 = (0.375 ms, −29.9 G/cm). Decoupling is interrupted during application of gradients (Kay, 1993). (b,c) ^{13}C$^{\alpha/\beta}$ 90° (180°) pulses (between points a and b) are applied with fields of $\Delta/\sqrt{15}$ ($\Delta/\sqrt{3}$) where Δ is the difference (Hz) between the carrier (43 ppm) and the center of the ^{13}CO chemical shift region (Kay et al., 1990), while shaped ^{13}CO 180° pulses have the SEDUCE-1 profile (McCoy and Mueller, 1992a) and are 225 μs in duration. The pulses marked with vertical arrows compensate for Bloch–Siegert effects (Vuister and Bax, 1992). At point b the carbon carrier is shifted to 58 ppm. All subsequent ^{13}C 90° (180°) pulses are applied with fields of $\Delta'/\sqrt{15}$ ($\Delta'/\sqrt{3}$) where Δ' is the difference (Hz) between the centers of the ^{13}CO and ^{13}C$^\alpha$ chemical shift regions. The delays used are: τ_a = 1.8 ms, τ_b = 1 ms, τ_c = 3.6 ms, τ_d = 2.7 ms, τ_e = 1.8 ms, T_C = 3.6 ms, ζ = 12.4 ms. The phase cycle employed is: ϕ1 = (x,−x), ϕ2 = 2(y),2(−y), ϕ3 = 4(x),4(−x), ϕ4 = 4(x),4(−x), ϕ5 = 8(x),8(−x), ϕ6 = 2(x),2(−x), rec = (x,−x,−x,x),2(−x,x,x,−x),(x,−x,−x,x). Quadrature detection in t_1 and t_2 is obtained by States-TPPI of ϕ1 and ϕ6, respectively. The strengths and durations of gradients are: g0 = (0.5 ms, 4 G/cm), g1 = (0.5 ms, 8 G/cm), g2 = (1 ms, 15 G/cm), g3 = (0.1 ms, 10 G/cm), g4 = (2.5 ms, 17 G/cm), g5 = (0.5 ms, 12 G/cm), g6 = (0.4 ms, 7.5 G/cm), g7 = (0.5 ms, 12 G/cm), g8 = (3.5 ms, 20 G/cm), g9 = (2 ms, 20 G/cm), g10 = (1.3 ms, 10 G/cm), g11 = (1.3 ms, 7 G/cm). Note that in both experiments correlations where magnetization originates on Gly residues are severely attenuated.

ponents contains a proline-rich region important for binding. These include the SH2 domain from the protein Crk, with a proline-rich insertion in the DE loop recognized by the SH3 domain from Abl kinase (Feller et al., 1994), as well as a complex of the C-terminal WW domain of rat Nedd4 and a proline-rich target

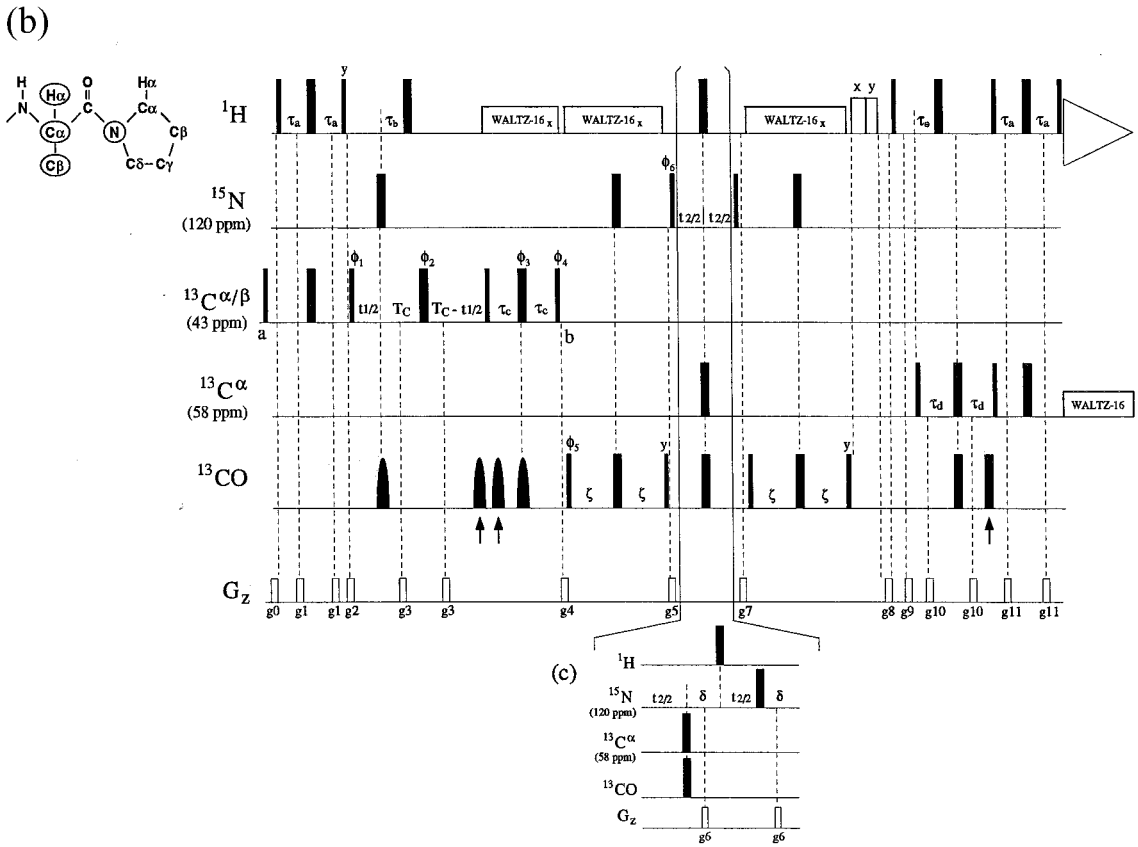

Figure 1. (continued).

sequence from the epithelial sodium channel (Staub et al., 1996; Staub and Rotin, 1996; Kanelis et al., 1998). Sequential assignment of the proline-rich regions in each case has been accomplished using a pair of pulse schemes which correlate (i) intra-residue $^1H^\alpha$, $^{13}C^\alpha/^{13}C^\beta$ chemical shifts with the ^{15}N shift of the subsequent residue [(HB)CBCA(CO)N(CA)HA] and (ii) intra-residue $^1H^\alpha$, $^{13}C^\alpha$, ^{15}N chemical shifts with the nitrogen shift of the next amino acid [HACAN]. These experiments supplement a number of schemes which exist in the literature for assignment of proline-containing regions in proteins. These include a sequence by Fesik and co-workers which correlates $^1H^\alpha$, $^{13}C^\alpha$ shifts of residues immediately preceding proline residues in ^{15}N, ^{13}C labeled proteins (Olejniczak and Fesik, 1994) as well as a sequence described by Bottomley et al. which links the $^{13}C^\alpha/^{13}C^\delta$ shifts of residue i with the $^{13}C^\alpha/^1H^\alpha$ shifts of the preceding residue i−1 (Bottomley et al., 1999). Herein brief descriptions of the pulse sequences described above for backbone assignment are presented along with applications to the Crk SH2 and WW domain complexes described above.

Results and discussion

Figure 1a illustrates the HACAN scheme that has been developed. The sequence is similar to a previously published HACAN scheme proposed by Bax and co-workers and only the differences will be described here. The transfer of magnetization proceeds as:

$$\begin{aligned} &^1H^\alpha(i) \xrightarrow{^1J_{H\alpha,C\alpha}} {}^{13}C^\alpha(i) \xrightarrow{^1J_{N,C\alpha},\,^2J_{N,C\alpha}} \\ &^{15}N(i),\ ^{15}N(i+1),\ t_1 \longrightarrow \\ &^{13}C^\alpha(i),\ \left[CT-t_2;\,^1J_{N,C\alpha},\,^2J_{N,C\alpha}\right] \xrightarrow{^1J_{H\alpha,C\alpha}} \\ &^1H^\alpha(i),\ t_3 \end{aligned} \tag{1}$$

where the active couplings involved in each transfer step are indicated and t_i (i = 1–3) denote acquisition periods. Fourier transformation of the resulting 3D

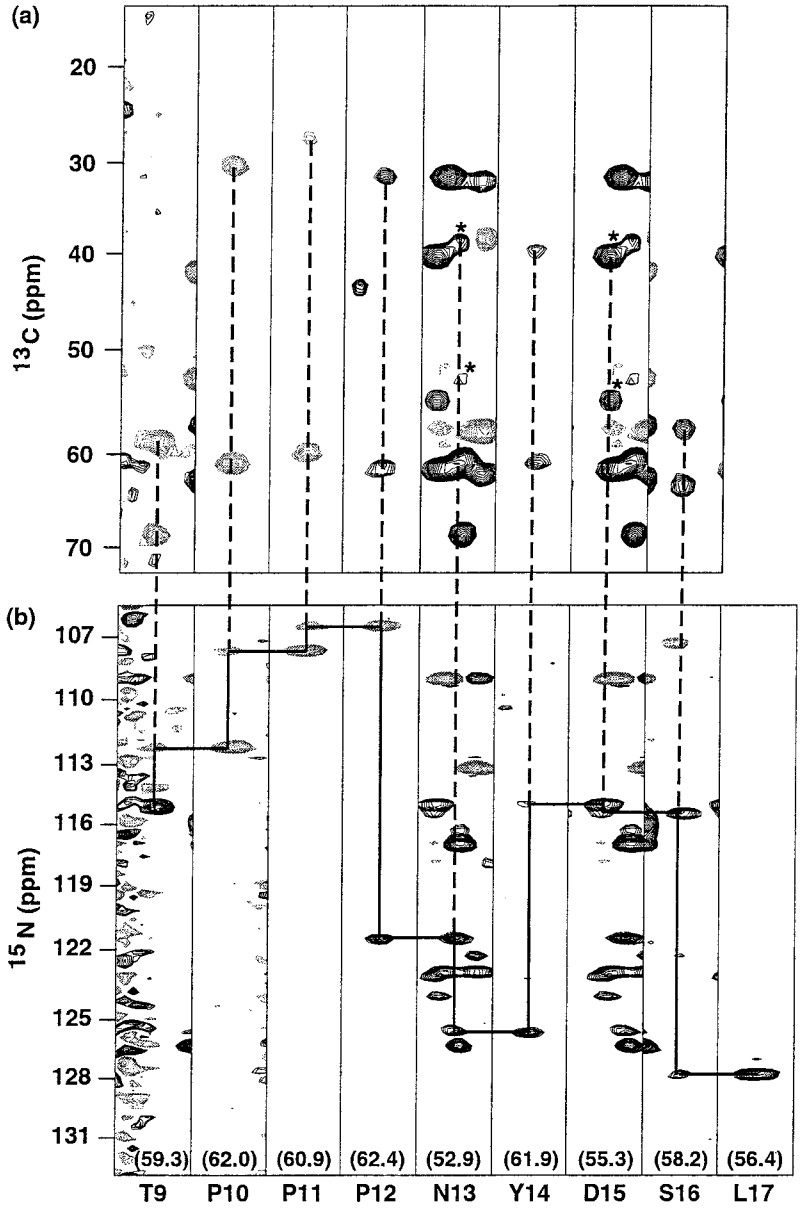

Figure 2. (a) Strips from the 2D (F_1/F_3) (HB)CBCA- (CO)N(CA)HA spectrum of the unlabeled C-terminal WW domain of rat Nedd4 with a ^{15}N, ^{13}C-labeled proline-rich target sequence (17 residues) from the epithelial sodium channel at the $^1H^{\alpha}$ chemical shift of the residue indicated along the x-axis. (b) Strips from the corresponding 2D (F_1/F_3) HACAN spectrum. Spectra were recorded on a sample of 3 mM unlabeled WW domain, 1 mM labeled peptide, 10 mM sodium phosphate, pH 6.5, 30 °C, 90% H_2O/10% D_2O on a Varian Inova 500 MHz spectrometer. Measuring times of approximately 1 h/2D spectrum were employed. In (a) the symbol * is used to indicate the position of correlations for N13 and D15. These data sets (and those in Figure 3) were processed using NMRPipe/NMRDraw (Delaglio et al., 1995) and analyzed using either the PIPP/CAPP (Garrett et al., 1991) or NMRView (Johnson and Blevins, 1994) programs. Negative contours are indicated by light shading.

Table 1. Examples of binding domains and proteins recognizing proline-rich regions

Protein	Domain	Target	Sequence
Grb2[a]	SH3	Sos1	VPPPVPPRR
Abl[b]	SH3	Crk	PRPPVPPSPAQPPP
Nedd4[c]	WW	α-ENaC	PPLALTAPPPAY
		β-ENaC	TLPTPGTPPPNYDSL
		γ-ENaC	PGTPPPRY
FBP11[d]	WW	ld10	PPLP
FE65[e]	WW	Mena	PPLP
FBP21[f]	WW	SmB and SmB′	PPPGMRPP
Profilin[g]		VASP site 1	LEGGGPPPPPALPTW
		VASP site 2	GPPAPPAGGPPPPPGPPPPPGPPPPPGLPPSG
		Mena site 1	SGPAAPPPPPPPPPPPPPPLPPPPLPPLASL
		Mena site 2	LGPPAPPPPPLPSGPAYSALPPPPGPPPPPPLPSTGPPPPPPPPPPLPNQA
		Cdc12p	IITHPTPPPPPPLP...PAFPPPPPPPPPPLVS
		formin site 1	PPAPPTPPPLPPPLIPPPPPLPPGL
		formin site 2	CPUSPPPPPPPPPPTPVPPSDGPPPPPPPPPPLPNVLA
		formin site 3	NSGGPPPPPPPPPPPP
Mena/VASP[h]	EVH1	vinculin	FPPPP
		zyxin	FPPPP
CD2BP2[i]	GYF	CD2	PPPPGHRSQAPSHRPPPPGHR

[a]Rozakis-Adcock et al., 1993; [b]Feller et al., 1994; [c]Staub et al., 1996; Staub and Rotin, 1996; [d]Bedford et al., 1997; [e]Ermekova et al., 1997; [f]Bedford et al., 1998; [g]Reinhard et al., 1995; Gertler et al., 1996; [h]Gertler et al., 1996; Niebuhr et al., 1997; [i]Freund et al., 1999.

time-domain matrix yields a data set with correlations at ($\omega_{N(i)}$, $\omega_{C\alpha(i)}$, $\omega_{H\alpha(i)}$) and ($\omega_{N(i+1)}$, $\omega_{C\alpha(i)}$, $\omega_{H\alpha(i)}$). This experiment is extremely valuable for proline-rich regions of proteins in that sequential correlations can be observed linking multiple proline residues, a situation that occurs with some frequency among proline-rich targets, as demonstrated in Table 1.

For the successful application of the present scheme to proteins and protein complexes on the order of 15–20 kDa, it is important that sensitivity be maximized. The main source of signal loss in this experiment stems from the efficient decay of transverse $^{13}C^{\alpha}$ magnetization during the T_C delays. In principle, therefore, it is important that these delays be optimized on a per-protein basis and that evolution due to passive couplings, $^1J_{C\alpha,CO}$ and $^1J_{C\alpha,C\beta}$, be completely refocused by the end of each $2T_C$ interval. Although a choice of $2T_C = 1/^1J_{C\alpha,C\beta}$ ensures that the signal intensity is not attenuated by $^{13}C^{\alpha}$–$^{13}C^{\beta}$ couplings (Santoro and King, 1992; Vuister and Bax, 1992), this value of T_C may be prohibitively long for many systems. Application of band-selective IBURP-2 inversion pulses (Geen and Freeman, 1991) centered at 30 ppm refocuses evolution from $^1J_{C\alpha,C\beta}$ couplings for the majority of residues in a protein, allowing a value of T_C to be chosen in a manner independent of $^1J_{C\alpha,C\beta}$. For example, a 1.8 ms pulse inverts ($M_z \longrightarrow >95\% -M_z$) $^{13}C^{\beta}$ signals resonating between 38.8 and 21.2 ppm (at 500 MHz), while signals downfield of 44 ppm are unperturbed ($< 3\%$). In the case of proline residues, with average random coil $^{13}C^{\alpha}$,$^{13}C^{\beta}$ shifts of 63 and 32 ppm (Wishart et al., 1995), respectively, this inversion profile is ideal. Sensitivity is also maximized in the present sequence by preserving both cosine- and sine-modulated t_2 components (Palmer et al., 1991) with coherence transfer selection by gradients (Kay et al., 1992; Schleucher et al., 1993), allowing spectra to be recorded in ^1H_2O.

The (HB)CBCA(CO)N(CA)HA sequence illustrated in Figure 1b generates cross peaks at ($\omega_{C\beta(i)}$/$\omega_{C\alpha(i)}$, $\omega_{N(i+1)}$, $\omega_{H\alpha(i)}$), allowing facile separation of intra- from inter-residue correlations in the HACAN. This experiment is very similar to the previously published (HB)CBCACO(CA)HA (Kay, 1993), with an additional transfer period in the present scheme to relay the magnetization to ^{15}N of residue i+1 from the ^{13}CO of i. It is possible to invert the sign of non-proline signals by allowing ^{15}N magnetization to evolve under the one-bond ^1HN-^{15}N scalar coupling, $^1J_{NH}$, for an additional period of $2\delta = 1/^1J_{NH}$, as il-

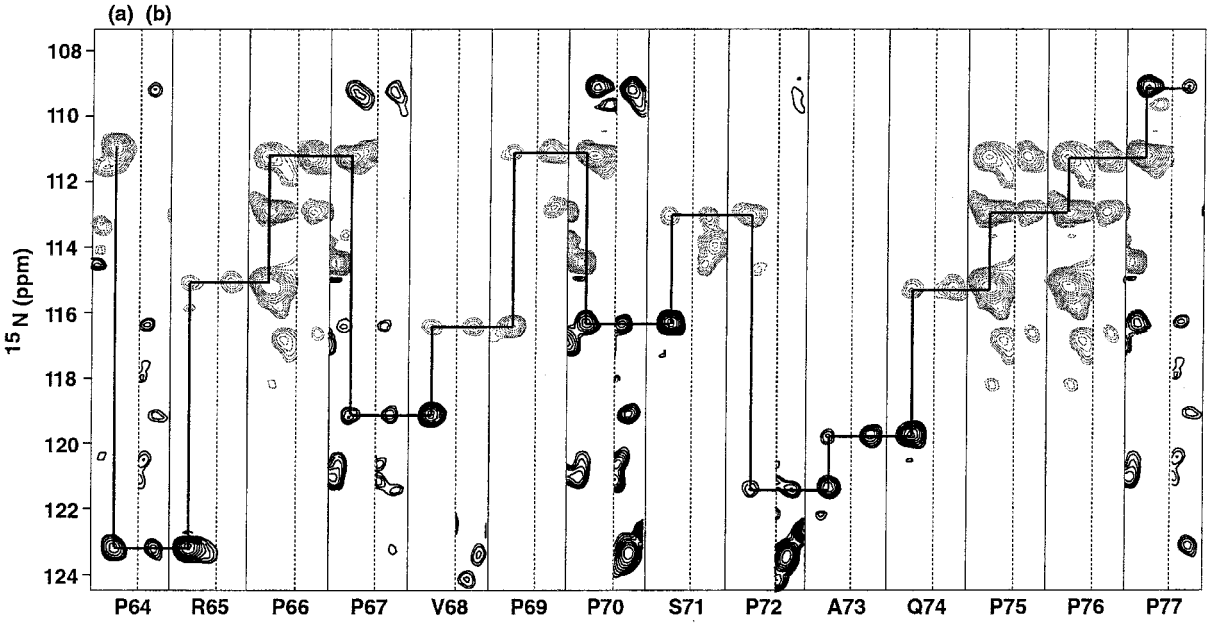

Figure 3. Strips from (a) 3D HACAN and (b) 3D (HB)CBCA(CO)N(CA)HA spectra taken at the $^{13}C^{\alpha}$,$^{1}H^{\alpha}$ chemical shifts of the residue indicated along the x-axis and recorded on a trimolecular complex comprising a ^{15}N, ^{13}C-labeled Crk SH2 domain, an unlabeled Crk phosphopeptide consisting of residues 217–229 of intact Crk and an unlabeled Abl SH3 domain in the ratio (1.0 mM, 1.1 mM, 1.1 mM). Buffer conditions are 50 mM sodium phosphate, pH 6.8, 0.01% sodium azide, 30 °C, 90% H_2O/10% D_2O. Spectra were recorded on a Varian Inova 500 MHz spectrometer. The HACAN data set was collected as a (32,58,512) complex matrix corresponding to acquisition times of (25.8 ms, 17.8 ms, 64 ms) in (t_1,t_2,t_3), while a (50,46,512) matrix [(6.4 ms, 37.5 ms, 64 ms)] was employed for the (HB)CBCA(CO)N(CA)HA.

lustrated in Figure 1c. Although the ^{15}N chemical shift for proline residues is distinctively downfield, the sign change relative to other correlations provides a useful confirmation of the assignment. Moreover, because proline residues lack an amide proton, the additional delay of $1/^{1}J_{NH}$ does not introduce significant relaxation losses for X-Pro correlations, at least for the proteins that we have examined.

Figure 2 illustrates the quality of data obtained from a complex of the unlabeled C-terminal WW domain of rat Nedd4 (50 residues) with a ^{15}N, ^{13}C-labeled proline-rich target sequence (17 residues) from the epithelial sodium channel (Staub et al., 1996; Staub and Rotin, 1996). Because the peptide is small, only 2D (F_1,F_3) spectra were necessary for assignment. In (a) strips from the (HB)CBCA(CO)N(CA)HA for a region extending from T9 to S16 are illustrated. Since data was recorded using the scheme of Figure 1c, correlations involving residues immediately preceding a proline are of opposite sign relative to those that are not. Figure 2b shows correlations from the HACAN from which sequential connectivities are readily obtained. Note that cross peaks derived from prolines are aliased in F_1 (^{15}N) and, because a first order phase correction of 180° is employed in this dimension, they are of opposite phase relative to other correlations.

Figure 3 shows strips from data recorded on a complex of ^{15}N, ^{13}C labeled Crk SH2 (120 residues), unlabeled Abl SH3 (65 residues) and an unlabeled 13 residue phosphorylated peptide comprising the region in Crk that binds its SH2 domain in an intramolecular fashion (Rosen et al., 1995). Slices from three-dimensional data sets recorded with the HACAN (a) and the (HB)CBCA(CO)N(CA)HA (b) schemes, respectively, are illustrated, taken at the $^{13}C^{\alpha}$, $^{1}H^{\alpha}$ chemical shifts of the residues indicated along the x-axis. The fact that assignments could be obtained for this region despite the large numbers of proline residues (9 of 14) and the degeneracy or near degeneracy of $^{13}C^{\alpha}$, $^{1}H^{\alpha}$ and ^{15}N shifts of P66, 75 and 76 is a good illustration of the utility of the HACAN and the (HB)CBCA(CO)N(CA)HA experiments.

Conclusions

In summary, a pair of pulse schemes have been presented that are particularly useful for the assignment

of backbone chemical shifts of proline residues in ^{15}N, ^{13}C labeled proteins. The experiments are also of value for applications to proteins dissolved at high pH, where assignment strategies based on recording ^{1}HN chemical shifts may fail.

Acknowledgements

The authors are grateful to Drs. Mike Rosen (Sloan Kettering) and Neil Farrow (Merck) for their participation in early stages of pulse sequence development many (!) years ago. This research was supported by a grant from the National Cancer Institute of Canada (J.D.F-K. and L.E.K). V.K. acknowledges support from an Ontario Graduate Predoctoral Fellowship. L.E.K. is an International Research Scholar of the Howard Hughes Medical Institute.

References

Alexandropoulos, K., Cheng, G. and Baltimore, D. (1995) *Proc. Natl. Acad. Sci. USA*, **92**, 3110–3114.

Bedford, M.T., Chan, D.C. and Leder, P. (1997) *EMBO J.*, **16**, 2376–2383.

Bedford, M.T., Reed, R. and Leder, P. (1998) *Proc. Natl. Acad. Sci. USA*, **95**, 10602–10607.

Bottomley, M.J., Macias, M.J., Liu, Z. and Sattler, M. (1999) *J. Biomol. NMR*, **13**, 381–385.

Delaglio, F., Grzesiek, S., Vuister, G.W., Zhu, G., Pfeifer, J. and Bax, A. (1995) *J. Biomol. NMR*, **6**, 277–293.

Ermekova, K.S., Zambrano, N., Linn, H., Minopoli, G., Gertler, F., Russo, T. and Sudol, M. (1997) *J. Biol. Chem.*, **272**, 32869–32877.

Feller, S.M., Knudsen, B. and Hanafusa, H. (1994) *EMBO J.*, **13**, 2341–2351.

Freund, C., Dötsch, V., Nishizawa, K., Ellis, L., Reinherz, E.L. and Wagner, G. (1999) *Nat. Struct. Biol.*, **6**, 656–660.

Garrett, D.S., Powers, R., Gronenborn, A.M. and Clore, G.M. (1991) *J. Magn. Reson.*, **95**, 214–220.

Geen, H. and Freeman, R. (1991) *J. Magn. Reson.*, **93**, 93–141.

Gertler, F.B., Niebuhr, K., Reinhard, M., Wehland, J. and Soriano, P. (1996) *Cell*, **87**, 227–239.

Johnson, B.A. and Blevins, R.A. (1994) *J. Biomol. NMR*, **4**, 603–614.

Kanelis, V., Farrow, N.A., Kay, L.E., Rotin, D. and Forman-Kay, J.D. (1998) *Biochem. Cell. Biol.*, **76**, 341–350.

Kay, L.E. (1993) *J. Am. Chem. Soc.*, **115**, 2055–2057.

Kay, L.E., Ikura, M., Tschudin, R. and Bax, A. (1990) *J. Magn. Reson.*, **89**, 496–514.

Kay, L.E., Keifer, P. and Saarinen, T. (1992) *J. Am. Chem. Soc.*, **114**, 10663–10665.

Marion, D., Ikura, M., Tschudin, R. and Bax, A. (1989) *J. Magn. Reson.*, **85**, 393–399.

McCoy, M.A. and Mueller, L. (1992a) *J. Am. Chem. Soc.*, **114**, 2108–2112.

McCoy, M.A. and Mueller, L. (1992b) *J. Magn. Reson.*, **98**, 674–679.

Niebuhr, K., Ebel, F., Frank, R., Reinhard, M., Domann, E., Carl, U.D., Walter, U., Gertler, F.B., Wehlend, J. and Chakraborty, T. (1997) *EMBO J.*, **16**, 5433–5444.

Olejniczak, E.T. and Fesik, S.W. (1994) *J. Am. Chem. Soc.*, **116**, 2215–2216.

Palmer, A.G., Cavanagh, J., Wright, P.E. and Rance, M. (1991) *J. Magn. Reson.*, **93**, 151–170.

Pawson, T. (1995) *Nature*, **373**, 573–580.

Reinhard, M., Giehl, K., Abel, K., Haffner, C., Jarchau, T., Hoppe, V., Jockusch, B.M. and Walter, U. (1995) *EMBO J.*, **14**, 1583–1589.

Rosen, M.K., Yamazaki, T., Gish, G.D., Kay, C.M., Pawson, T. and Kay, L.E. (1995) *Nature*, **374**, 477–479.

Rozakis-Adcock, M., Fernley, R., Wade, J., Pawson, T. and Bowtell, D. (1993) *Nature*, **363**, 83–85.

Santoro, J. and King, G.C. (1992) *J. Magn. Reson.*, **97**, 202–207.

Schleucher, J., Sattler, M. and Griesinger, C. (1993) *Angew. Chem. Int. Ed. Engl.*, **32**, 1489–1491.

Shaka, A.J., Keeler, J., Frenkiel, T. and Freeman, R. (1983) *J. Magn. Reson.*, **52**, 335–338.

Staub, O., Dho, S., Henry, P., Correa, J., Ishikawa, T., McGlade, J. and Rotin, D. (1996) *EMBO J.*, **15**, 2371–2380.

Staub, O. and Rotin, D. (1996) *Structure*, **4**, 495–499.

Vuister, G.W. and Bax, A. (1992) *J. Magn. Reson.*, **98**, 428–435.

Wang, A.C., Grzesiek, S., Tschudin, R., Lodi, P. and Bax, A. (1995) *J. Biomol. NMR*, **5**, 376–382.

Wishart, D.S., Bigam, C.G., Holm, A., Hodges, R.S. and Sykes, B.D. (1995) *J. Biomol. NMR*, **5**, 67–81.

Yu, H., Chen, J.K., Feng, S., Dalgarno, D.C., Brauer, A.W. and Schreiber, S.L. (1994) *Cell*, **76**, 933–945.